BOLETIN DE LA SOCIEDAD ESPAÑOLA DE
Cerámica y Vidrio
www.elsevier.es/bsecv

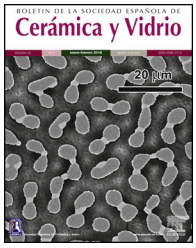

Original

Glass with a low-melting temperature belonging to the P_2O_5–CaO–Na_2O system, applied as a coating on technical ceramics (alumina, zirconia) and traditional ceramics (porcelain stoneware)

Luis Antonio Díaz[a], *Marta Suárez*[a], *Jose Florindo Bartolomé*[b,*], *Sonia Lopez-Esteban*[b], *Belén Cabal*[a], *Arnaldo Moreno*[c], *María del Carmen Bordes*[d], *Adolfo Fernández*[a], *Carlos Pecharromán*[b], *José Serafin Moya*[a]

[a] *Centro de Investigación en Nanomateriales y Nanotecnología (CINN) (CSIC-UNIOVI-PA), Consejo Superior de Investigaciones Científicas, Universidad de Oviedo, Principado de Asturias, Avda. de la Vega, 4-6, 33940 El Entrego, Asturias, Spain*
[b] *Instituto de Ciencia de Materiales de Madrid (ICMM – CSIC), Consejo Superior de Investigaciones Científicas, Calle Sor Juana Inés de la Cruz, 3, 28049 Madrid, Spain*
[c] *Instituto de Tecnología Cerámica (ITC), Universidad Jaime I, Campus Universitario Riu Sec, Avinguda de Vicent Sos Baynat, s/n, 12006 Castellón de la Plana, Castellón, Spain*
[d] *Instituto de Tecnología Cerámica (ITC), Asociación de Investigación de las Industrias Cerámicas (AICE), Universidad Jaime I, Campus Universitario Riu Sec, Avinguda de Vicent Sos Baynat, s/n, 12006 Castellón de la Plana, Castellón, Spain*

ARTICLE INFO

Article history:
Received 10 May 2023
Accepted 18 July 2023
Available online 3 August 2023

Keywords:
Low-melting point
Lead-free glass
Coating
Alumina
Circona
Porcelain stoneware

ABSTRACT

This article investigates the development and potential applications of low-melting point lead-free glasses. Their importance is due to strong market demands to comply with the strict international regulations against the use of lead. In this work, a preliminary study of the existing interactions of a low-melting-temperature glass belonging to the P_2O_5–CaO–Na_2O system when it is deposited on different ceramic substrates, both traditional (porcelain stoneware) and technical (alumina and zirconia), has been carried out. The ionic diffusion through the studied interfaces, the phases present, the composition of the glassy phase and the surface morphology of the coating have been studied by Field Emission Scanning Electron Microscopy (FESEM), with coupled EDX microanalysis. The chemical resistance of the different glassy coatings obtained is also evaluated. The results showed that these new lead-free low-melting-temperature glassy coatings are chemically and mechanically compatible, and promising candidates for applications and markets in a broad range of fields.

* *Corresponding author.*
E-mail address: jbartolo@icmm.csic.es (J.F. Bartolomé).
https://doi.org/10.1016/j.bsecv.2023.07.003

Vidrio de baja temperatura de fusión perteneciente al sistema P_2O_5-CaO-Na_2O, aplicado como revestimiento sobre cerámica técnica (alúmina, circona) y tradicional (gres porcelánico)

Palabras clave:
Bajo punto de fusión
Vidrio libre de plomo
Recubrimiento
Alúmina
Circona
Gres porcelánico

RESUMEN

Este artículo investiga el desarrollo y aplicaciones potenciales de los vidrios sin plomo de bajo punto de fusión. La importancia de estos materiales se debe a las fuertes demandas del mercado por las estrictas normativas internacionales contrarias a la utilización del plomo. En este trabajo se ha realizado un estudio preliminar de las interacciones existentes de un vidrio de baja temperatura de fusión, perteneciente al sistema P_2O_5-CaO-Na_2O, cuando se deposita sobre diferentes sustratos cerámicos tanto tradicionales (gres porcelánico) como técnicos (alúmina y circona). Mediante un estudio por microscopía electrónica de barrido con emisión de campo (FESEM) con microanálisis EDX acoplado, se han evaluado la difusión iónica a través de las interfases estudiadas, las fases presentes, la composición de la fase vítrea y la morfología superficial del recubrimiento. Además, se ha evaluado la resistencia química de los recubrimientos vítreos obtenidos. Los resultados muestran que son química y mecánicamente compatibles con las cerámicas tradicionales y técnicas. Estos resultados convierten a estos vidrios sin plomo y de baja temperatura de fusión en prometedores candidatos para un amplio rango de aplicaciones y mercados.

Introduction

The most important challenge nowadays in the field of low-melting glass materials (softening temperatures < 600 °C) – a consolidated and key technology for a wide range of industrial and consumer products – is to obtain ecofriendly alternatives to lead-containing glass products.

Currently, technology includes uses for sealing applications for electronics [1–3] as a glass matrix for thick-film materials (circuit carrier) and passive components (resistors, condensers, resonators, etc.), for encapsulation of organic light emitting diode (OLED) [4] and many microelectromechanical system (MEMS) devices [5–7], such as resonators, gyroscopes and tunnelling sensors. While most low-melting glasses are used for sealing, there are several significant applications for fuel cells, systems in solar energy devices, nuclear waste immobilization, together with overglazing of automotive, packaging and architectural glass [8].

The most classical low-melting glass materials based on the PbO–B_2O_3 system integrated in commercial devices present an important environmental impact due to the high toxicity of the lead oxide (PbO). Sources of contamination are the material components and waste generated during mechanical and other types of post-processing of the product, making its replacement necessary as also indicated in the directives adopted by the European Union (EU) for the exclusion or substitution of hazardous substances in electrical and electronic devices [9,10]. Accordingly, lead-free low-melting point glasses have a wide range of applications and great prospective future in electronic industry because of their low sealing temperature and respect for the environment.

On the other hand, it is not environmentally friendly to use a large amount of energy in processing materials at high temperature. Specifically, energy saving is an important issue with different approaches, from glass to ceramic industry sector. All these industries are characterized by the prolonged operation of high-temperature kilns and furnaces; not only a large amount of energy is consumed during the production process, but also the energy cost is a significant percentage of the total production costs. The implementation of energy saving technologies, therefore, is imperative for reasons that have to do both with the worldwide energy crisis and environmental degradation, as well as with product cost reduction. In this regard, the tile industry dominates the ceramic sector and is the most competitive, demanding the lowest production costs and the highest productivity [11]. A great quantity of thermal energy is consumed in ceramic tile manufacture, mainly in the firing stage. In fact, producing just one tonne of ceramic tiles requires 1.67 MWh of energy [12]. Reducing the environmental impact can be achieved by modifying the compositions of low-melting glass materials while maintaining their functional characteristics or by improving their manufacturing technology process, associated with lowering of firing temperatures.

In this context, many researchers have been investigating lead-free low-melting glass systems alternatives, for example ZnO–B_2O_3, R_2O–Sb_2O_3 (R = Li, Na, K), BaO (SrO, CaO)–Bi_2O_3–B_2O_3, SnO–ZnO–P_2O_5, R_2O–ZnO–P_2O_5, and others [13–25]. Zinc-borate glasses exhibit high softening temperatures in the range >600 °C. Antimony oxide presents high volatility, which complicates the synthesis of these glasses with low chemical stability. Bismuth borate glasses show low electric insulation properties. Most phosphate glasses do not satisfy the requirements in terms of chemical stability or they are characterized by heightened values of the softening temperatures.

In this work, the interactions between a low-melting glass coating belonging to the P_2O_5–CaO–Na_2O system, on different

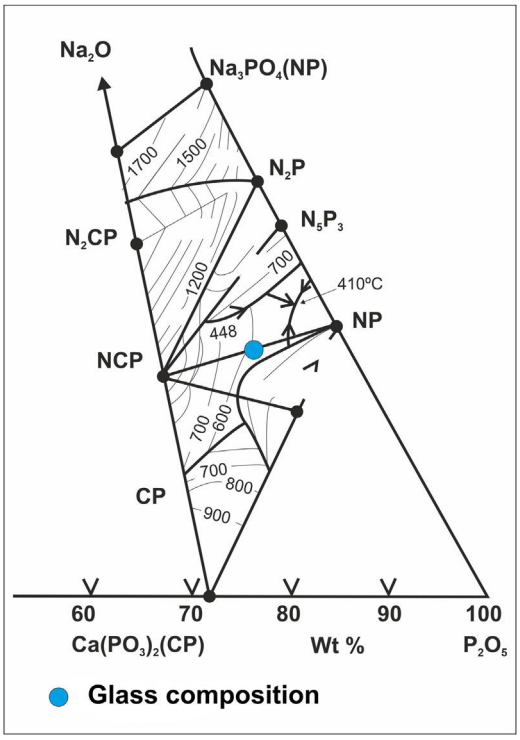

Fig. 1 – Location of the composition of glass within the ternary system P_2O_5–CaO–Na_2O.

advanced technical and traditional ceramic substrates have been studied. During the heat treatment, the glaze must be considered as a heterogeneous system changing its aggregation state, that is accompanied by structural modifications of the formed melt and of its phase composition as well. The final objective will be to evaluate whether the new designed glasses Pb-free satisfy both the low processing temperature and the mechanical and chemical compatibility requirements.

Methodology and materials

Glass preparation

Glass belonging to the ternary system P_2O_5–CaO–Na_2O [13] was synthesized starting from the mixture of 83 wt.% of sodium hexametaphosphate ($Na_{15}P_{13}O_{40}$, Sigma–Aldrich) and 17 wt.% of dicalcium phosphate ($CaHPO_4{\cdot}2H_2O$, Sigma-Aldrich), being its chemical composition (% in weight) the following: 65.60% P_2O_5, 5.76% CaO and 28.64% Na_2O. The precursors were weighed in a Pt–10% Rh crucible. The final heat treatment to melt the mixture was at 900 °C for 1 h stay. The melt was cooled by pouring it into a water-cooled stainless-steel container. In Fig. 1, the situation of the composition obtained within the ternary system can be seen.

The glass was ground and sieved below 63 μm and then deposited on each of the corresponding ceramic surfaces. The amount of the glass powder deposited on each of them was always controlled to be 0.05 g/cm^2. On the other hand, another glass has also been formulated to which 1 wt.% Co_2O_3 (Panreac, Spain) was added to achieve a blue colouration in the final glassy coating.

Table 1 – Solutions and residence times used for the determination of chemical resistance.

Test solution	Test time
Acids and bases (weak concentrations)	
Hydrochloric acid (dens. 1.19 g/ml) 3%	96 h
Citric acid 100 g/l	24 h
Potassium hydroxide 30 g/l	96 h

Characterization of the glass

For the characterization of the glass, X-ray diffraction (Bruker D8-Discover, UK) using Cu radiation (Kα) was used. The glass characteristic temperatures were analyzed by differential thermal analysis (DTA, TA Instruments, Q600, USA) with a heating rate of 10 °C/min up to 650 °C. In addition, the thermal characterization was also performed by Hot Stage Microscopy (HSM) using a side view optical microscope EM 201 with a computerized image analyser system and an electrical furnace Leica 1750/15. The powder glass samples were cold pressed in cylindrical dimensions (2 mm × 4 mm), and the measurements were conducted in air and with a 10 °C/min heating rate up to the flow temperature, using a ceramic support containing a Pt/Rh (6/30) thermocouple. The temperatures corresponding to the characteristic viscosity points (first shrinkage, maximum shrinkage, softening, half ball and flow) were obtained from the photomicrographs taken during the hot-stage microscopy experiment following the standards DIN 51730-1998 and ISO 540-1995. Additionally, the HSM software calculates the percentage of decrease in area of the sample images. The coefficient of thermal expansion of the glass was calculated using a dilatometry equipment (Netzsch DIL402C, Germany).

Different disks of technical ceramic with density > 99% have been used as substrates: (i) TM-DAR alumina (99.9% purity) from Taimei (Japan), and (ii) PSZ magnesia-doped zirconia (3% mol) from Unitec Ceramics (USA). Also, commercial glazed porcelain stoneware slabs (Castellón, Spain) were used. The study by microscopy and semi-quantitative microanalysis was carried out in a FESEM (FEI: Quanta FEG 650, USA). Previously, after their heat treatments, the specimens were first cross-sectioned, then prepared with SiC papers (4000) and, finally, polished with diamond cloths down to 6 and 3 μm. All the specimens were metallized with a nanometer layer of carbon for their observation by FESEM and subsequent microanalysis by EDX.

The chemical resistance was evaluated following the method described in the UNE-EN ISO 10545-13:2017 standard [26], which consists in the application of a certain volume of reagent on the surface of the tiles during a certain time. The concentration of the solutions used and their residence time on the specimens to be tested are detailed in Table 1.

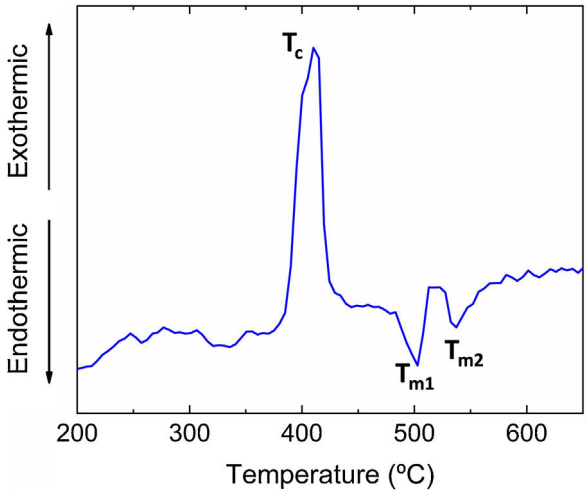

Fig. 2 – DTA curves obtained for the glass showing the exothermic crystallization temperature peak (T_c) and endothermic melting temperature peaks (Tm1 and Tm2).

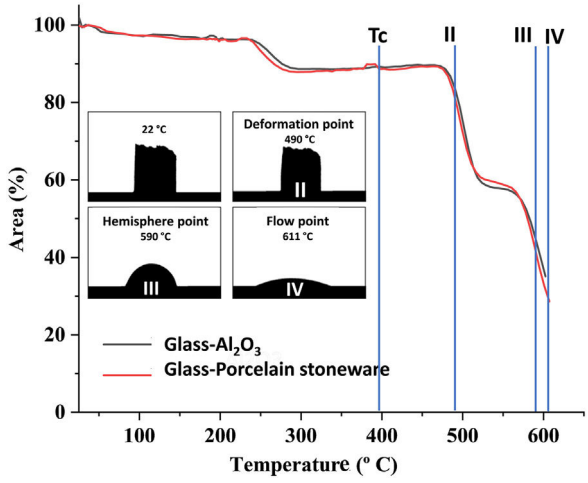

Fig. 3 – Variation in area of glass samples on the two types of substrates (alumina and porcelain), and photomicrographs of the shape glass sample evolution during the HSM measurement.

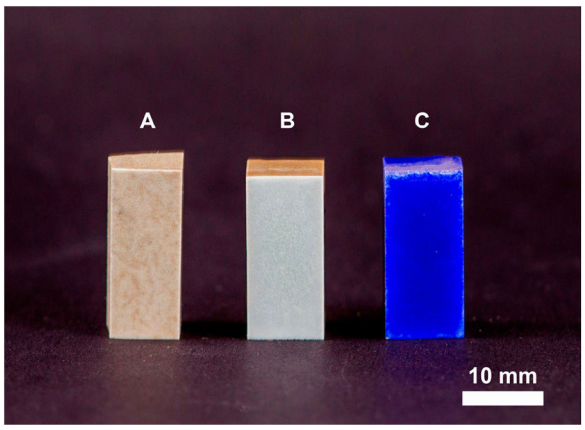

Fig. 4 – Glass coatings on porcelain tile. (A) Aspect of the uncoated porcelain tile, (B) coating under a heat treatment of 875 °C/2 h, and (C) coating with the glass doped with cobalt oxide and under the same heat treatment (875 °C/2 h).

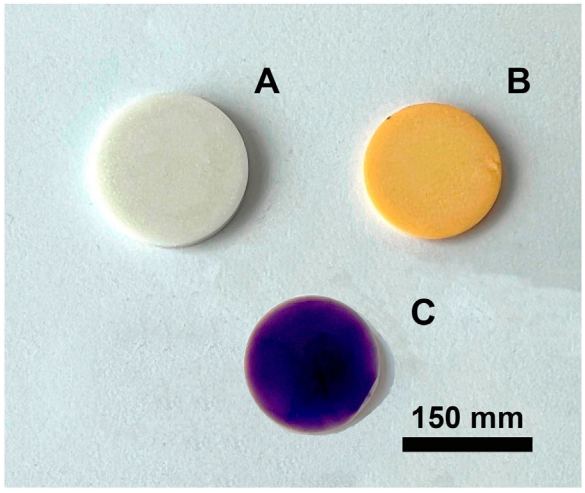

Fig. 5 – Glass coatings on alumina disks (A), zirconia 3% mol MgO disks (B) and glass doped with 1% weight of cobalt oxide on a zirconia–magnesia substrate (C). The heat treatment carried out was 775 °C/4 h.

Results

The differential thermal analysis (DTA) curve is shown in Fig. 2. The exothermic signal at ~425 °C can be ascribed to the crystallization of the glass (T_c). The two endothermic peaks (Tm1 and Tm2) at 500 and 550 °C are attributed to the melting of crystalline phases precipitated during the heating of the glasses. These values are in good agreement with the DTA results obtained in a similar glass composition studied in a previous work [13], where the exothermic crystallization and endothermic melting temperature peaks were found to be $T_c = 435$ °C and $T_m = 530$ °C, respectively.

In Fig. 3, the decrease in the area of the sample as a function of the temperature may be observed. The glass crystallization temperature of the glasses, T_c, obtained by DTA measurements is indicated. Complete densification takes place before the crystallization temperature. Additionally, the micrographs of the specimens resulting from the hot stage microscopy tests have been included in the figure, and record the main variations in their physical profile with increasing temperature. The temperature values at which softening (490 °C), half ball (590 °C) and flow (611 °C) take place are shown. The shrinkage points were not detected in these experimental conditions, as no physical changes are visible from the initial stage until the softening point.

Figs. 4 and 5 show the macro-surface appearance of the glass coatings on the different substrates tested. Two heat treatments were carried out: at 775 °C and 875 °C with residence times of 2 and 4 h. In Fig. 4A, the glass deposited on the porcelain stoneware can be observed. A colour change can be seen in Fig. 4B (white colour) and C (blue colour). In the case of technical ceramics (Fig. 5), the glass coating is transparent and,

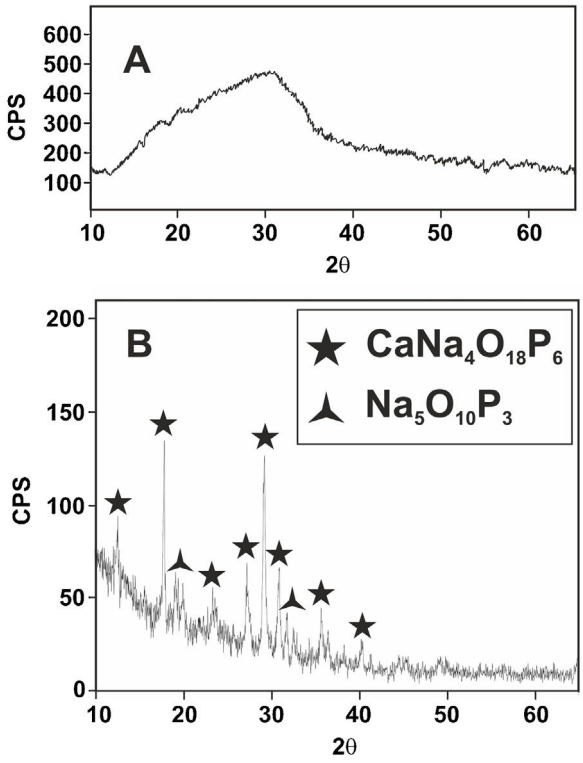

Fig. 6 – X-ray diffractogram of the: (A) synthesized glass and (B) heat-treated glass at 875 °C/2 h and cooled into the furnace at 1 °C/min.

therefore, the white colour of the alumina substrate (Fig. 5A) and the yellow colour of the zirconia substrate (Fig. 5B) are visible. In Fig. 5C, the glass doped with 1% weight of cobalt oxide, showing the typical blue colouration, on a zirconia–magnesia substrate is shown.

Fig. 6 shows the X-ray diffractogram of the glass, where the typical hump of amorphous materials can be seen. For comparison purposes, the XRD pattern of this glass after a heat treatment at 875 °C for 2 h and cooled into the furnace at a slow speed of 1 °C/min is also shown. A calcium sodium phosphate, $CaNa_4O_{18}P_6$, precipitates as the majority phase in good agreement with the equilibrium diagram of Fig. 1.

In Fig. 7, the microstructure of the cross section of the glassy coating on the alumina plate can be seen. The melt fits perfectly to the alumina surface, being the heat treatment used 775 °C/2 h. EDX microanalysis shows the presence of a small proportion of Al in the upper layer (Fig. 7, microanalysis 1) coming from the substrate, which results in the bright whitish colour of the surface, while in the lower layer, pure alumina, no cation coming from the coating is detected. The presence of superficial crack patterns on the coating surface can be observed.

The cross section of the 3 wt.% MgO zirconia substrate coated with the glass doped with 1 wt.% cobalt oxide is shown in Fig. 8. The heat treatment corresponding to this sample was 875 °C/2 h. As can be seen in the micrograph (Fig. 8A), a neat contact between the ceramic substrate and the glass coating can be observed, as well as idiomorphic crystals rich in calcium phosphate that appear in the contact zone. EDX microanalyses taken in different areas are plotted in Fig. 8.

Regarding the coating of porcelain tile with glass, a study of the interactions between the two materials was carried out, taking into account two heat treatments at 775 °C and 875 °C and with two final holding times: 2 h and 4 h. Figs. 9 and 10 show the microstructures of the polished cross-sections of the heat treatments carried out at 775 °C with 2 h and 4 h of holding time.

Referring to Fig. 9, it is noteworthy that the layer of glass fits perfectly to the relief of the original porcelain substrate; however, after the heat treatment for 2 h, its chemical composition changes compared to the original one. Thus, throughout the thickness, it can be seen that there has been a microdiffusion of ions rich in silica and also in aluminium from the glaze substrate of the starting porcelain.

In Fig. 10, other microstructures can be observed by FESEM under the same heat treatment, but with a residence time twice as long as the previous one: 4 h. This figure shows the average chemical composition of the engobe-glaze assembly and the chemical composition of the starting glass (Fig. 10A). In Fig. 10B, the microstructure of the glazed layers can be seen in detail, where in the contact zone of the glass coating on the porcelain tile substrate, there are two compositional zones due to the existing reactions and the subsequent diffusion of the cations present in both the porcelain tile glaze and its engobe. Specifically, there is a layer of about 60–65 μm where there is an important fraction of cations (Al, Si, Mg, K, Ba and Zn) that are not present in the original composition of the glass, which are responsible for the whitish colouration of the final glaze (Fig. 4B). The other continuous layer below of about 25 μm is rich in Si, and is the result of the reorganization of the dark grey precipitates (Fig. 9A) with increasing holding time of the heat treatment. EDX microanalyses corroborate this fact as can be seen in positions (1)–(3) of Fig. 10.

The pieces thermally treated at 875 °C/4 h were considered to be tested against both acid and alkaline attack, according to the conditions established by standards ISO 10545. In Fig. 11, the surface appearance of the treated pieces can be observed, where the treatments with citric acid and potassium hydroxide seem unalterable after being washed. On the other hand, when the attack with hydrochloric acid is evaluated, a superficial deterioration is observed with loss of shine of the piece. The results showed that the coating exhibits chemical stability at an acceptable level.

Discussion

In this work, a Pb-free low-melting point glass with an environmentally compatible non-toxic chemical composition has been selected [13]. As shown in Fig. 2, this glass has an endothermic melting temperature peaks in the DTA located at 500 °C and 550 °C. Additionally, a flow point is reached at 611 °C, regardless of the support substrate on which the high-temperature optical microscopy test has been carried out (alumina, porcelain). For this reason, and taking into account the Stokes–Einstein equation [27] ($D \approx K_B\, T/\lambda\eta$, where D is the diffusivity; K_B is the Boltzmann constant, T is the temperature (K); λ is the diameter of the diffusing molecule;

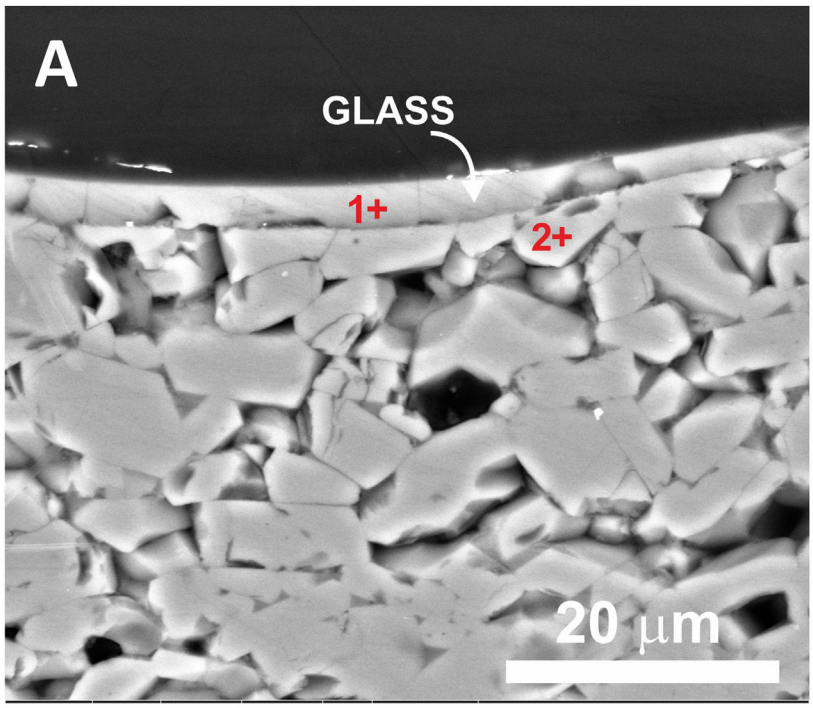

①

Element	Wt%	At%
CK	23.66	36.72
OK	26.68	31.08
NaK	10.01	08.11
AlK	09.53	06.59
PK	25.53	15.36
CaK	04.59	02.13
Matrix	Correction	ZAF

②

Element	Wt%	At%
CK	13.19	21.72
OK	29.01	35.88
AlK	57.81	42.40
Matrix	Correction	ZAF

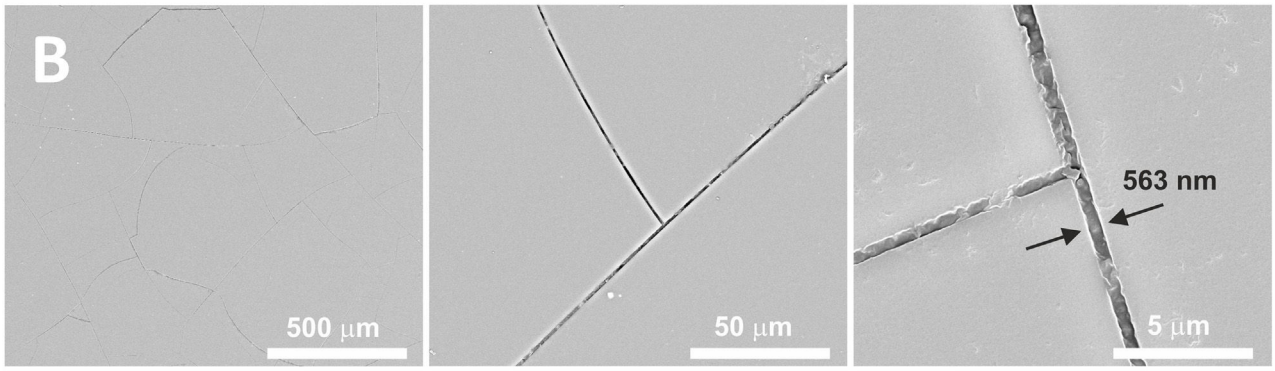

Fig. 7 – (A) FESEM observation and EDX analysis of the cross section of the glass on the alumina disc. The heat treatment performed was at 775 °C/2 h. (B) Surface of the coated sample at different magnifications. The presence of micro-cracks due to the stresses generated by the different coefficients of thermal expansion between the substrate and the coating can be observed.

η is the viscosity), the heat treatment temperature for the coatings was chosen to be around 200 °C above the mentioned fluidity temperature (775–875 °C), in order to facilitate the diffusion and exchange of ions through the coating/substrate interface and, consequently, to be able to modify their chemical composition and increase its chemical stability.

This transfer of ions at the glass/substrate interface has been widely achieved in the temperature range studied. As can be seen in Fig. 7, in the case of the alpha-alumina substrate at 775 °C, alumina dissolution has been produced at the interface, which has been incorporated into the glass composition (≈6.6 Al at.% was detected) making it more durable than traditional phosphate glasses [28]. In this particular case, the presence of surface microcracking is due to the large difference between the coefficients of thermal expansion of the alumina substrate ($7.2 \times 10^{-6}\,°C^{-1}$) and the glass coating ($24 \times 10^{-6}\,°C^{-1}$) [29].

In the case of the Mg–Zirconia substrate (Fig. 8), a perfect glass–ceramic adhesion, free of microcracks, is observed. A precipitation of isomorphic crystals of calcium and sodium phosphate along the interface, with sizes ranging between 0.1 and 1 μm, is detected. This fact is in good agreement with the equilibrium diagram of Fig. 1 and with the X-ray diffraction pattern of the original glass thermally treated at 875 °C for 2 h (Fig. 6). The composition of the glassy phase was notably modified, drastically decreasing its Na_2O and P_2O_5 content, as can be seen in the corresponding EDX analyses. Such effect induces a greater resistance to chemical attack of the final glaze obtained. In this particular case, because of the higher value of the thermal expansion coefficient of the PSZ substrate

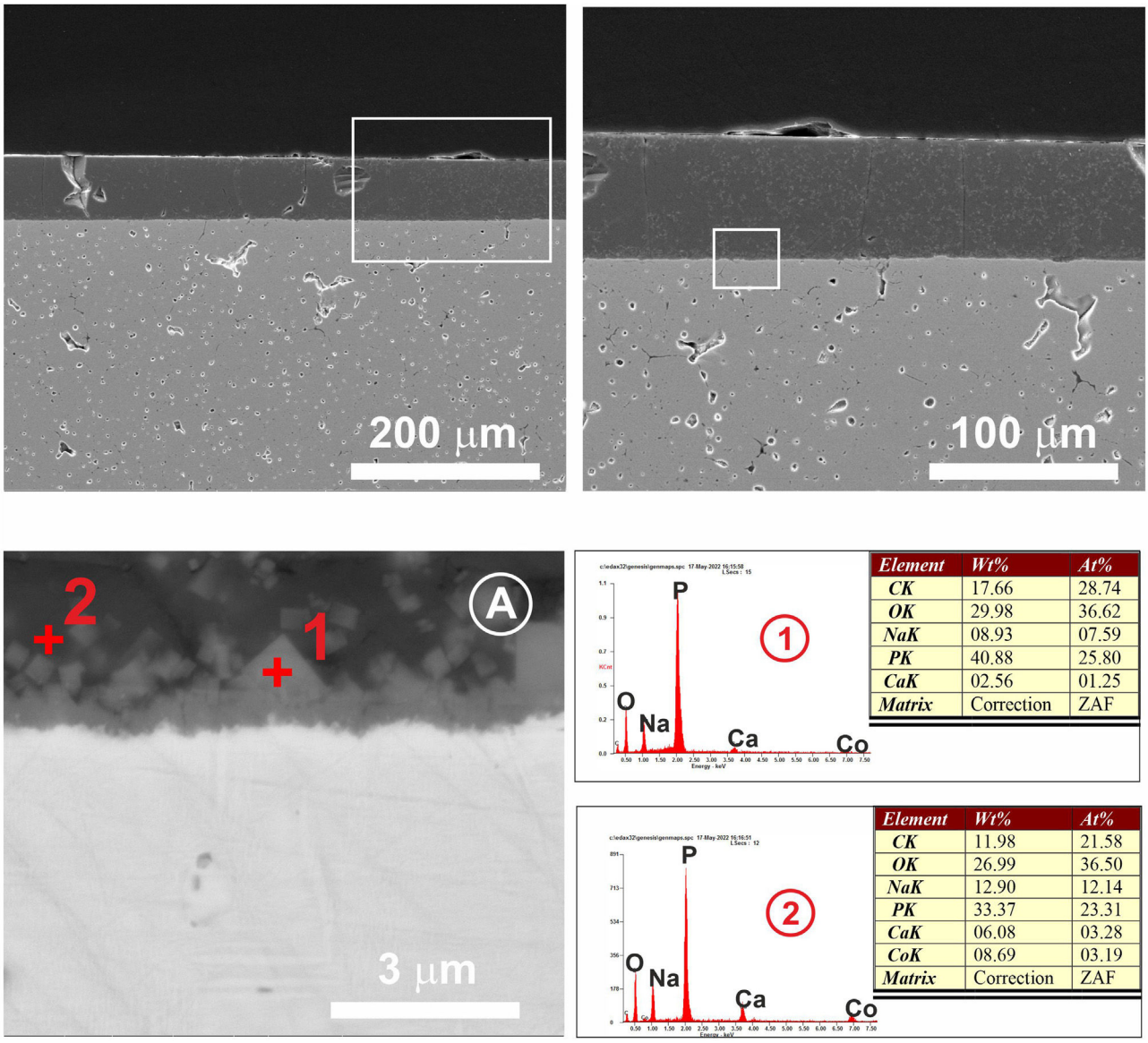

Element	Wt%	At%
CK	17.66	28.74
OK	29.98	36.62
NaK	08.93	07.59
PK	40.88	25.80
CaK	02.56	01.25
Matrix	Correction	ZAF

Element	Wt%	At%
CK	11.98	21.58
OK	26.99	36.50
NaK	12.90	12.14
PK	33.37	23.31
CaK	06.08	03.28
CoK	08.69	03.19
Matrix	Correction	ZAF

Fig. 8 – Cross section at different magnifications of the 3 wt.% MgO zirconia substrate coated with the glass doped with 1 wt.% cobalt oxide. EDX microanalyses taken in different areas of the interface are showed. In (A) the calcium phosphate microcrystals can be seen in the contact zone between the two dissimilar surfaces.

($11 \times 10^{-6}\,^{\circ}C^{-1}$), an excellent adhesion is achieved, and also a good mechanical coupling that prevents the appearance of superficial microcracks. Furthermore, through a detailed observation of the glassy coating/PSZ interface shown in the SEM micrographs of Fig. 8, it can be deduced that the zone of approximately 30 μm deep of the zirconia substrate in contact with the coating is apparently denser and more absent of pores than the rest of the substrate. This fact could be due to a diffusion/wetting process of the glassy phase of the coating through the zirconia grain boundaries improving the anchorage of the coating as well as its mechanical stability.

In the case of porcelain tile, the substrate on which this low-melting point glass has been deposited, corresponds to a commercial ceramic glaze with a high silica and alumina content (≈50 wt.%, 22 wt.%, respectively). Therefore, in this particular case there is a high driving force $\Delta G < 0$ that favours the diffusion of the Si^{4+} and Al^{3+} ions from the ceramic glaze to the glass at the interface, as clearly observed in the FESEM micrographs corresponding to the cross section of the glass/porcelain tile treated at 775 °C (Figs. 9 and 10). In these figures a high concentration of silica at the glass/glaze interface can be seen. The Si^{4+} has migrated from the original glaze to the glass. This silica-rich layer precipitates probably in the form of cristobalite [30] when it reaches a certain concentration, reorganizes and increases its thickness during the heat treatment, reaching about 25 μm after 4 h. The composition of the top glassy phase has been significantly modified with Al, Ba and Zn ions (according to the EDX analysis), which have

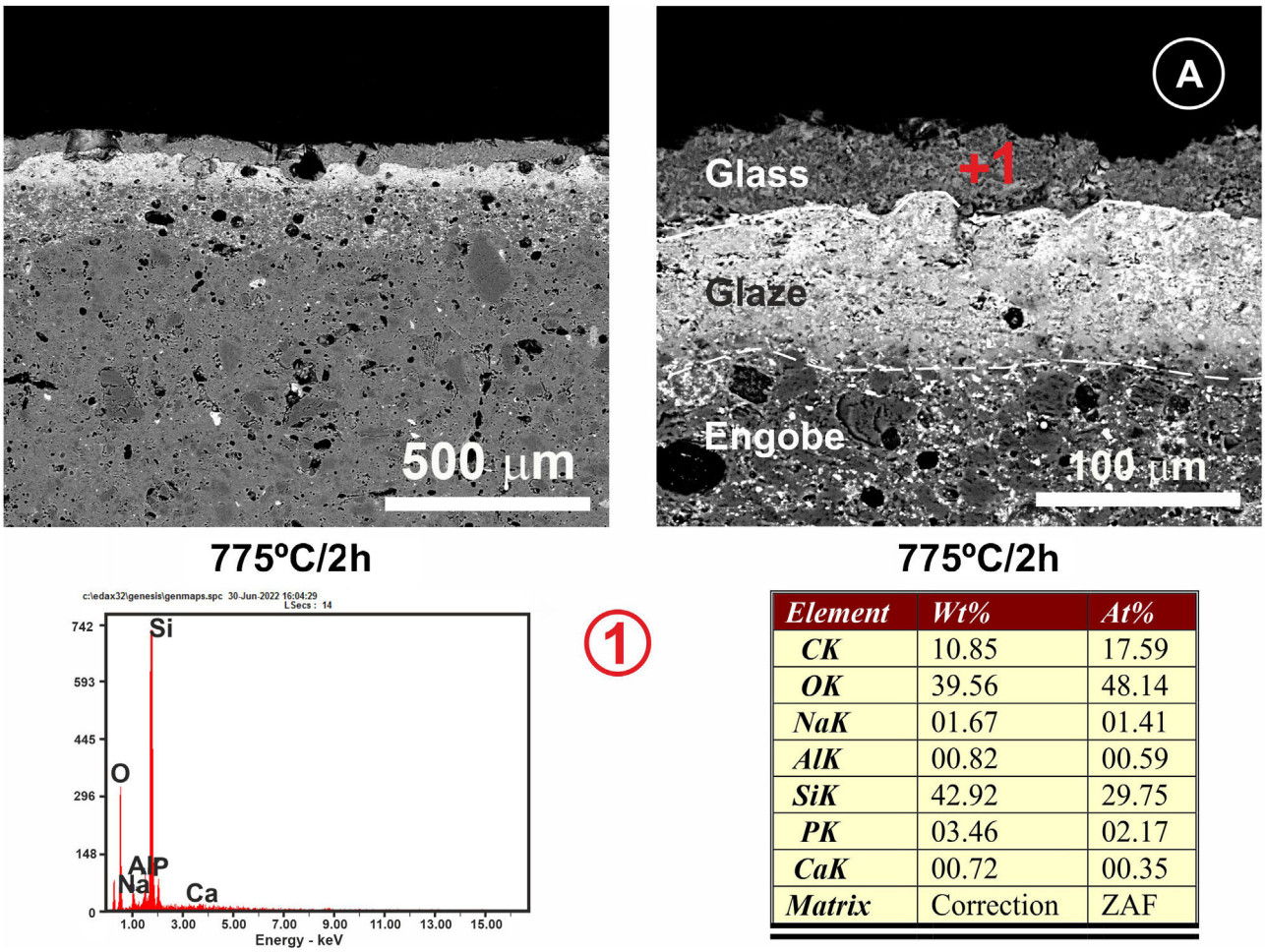

Element	Wt%	At%
CK	10.85	17.59
OK	39.56	48.14
NaK	01.67	01.41
AlK	00.82	00.59
SiK	42.92	29.75
PK	03.46	02.17
CaK	00.72	00.35
Matrix	Correction	ZAF

Fig. 9 – FESEM micrographs and EDX microanalyses corresponding to the cross section of the glass/porcelain tile treated at 775 °C/2 h.

migrated from the original glaze of the porcelain tile. Due to this ionic interdiffusion, it has been possible to modify the original composition of the glass during the heat treatment. Taking into account that the chemical stability of phosphate glass is generally poor, that greatly limits its applications [31]. This fact allows to improve its chemical stability, for instance to the citric acid and the alkaline one, as can be seen from the tests of resistance to chemical attack (Fig. 11). Therefore, the ionic interdiffusion data obtained in this work open up the possibility of designing *ad hoc* compositions that can satisfy the strict requirements of applications with higher added values, e.g. microelectronics, surface decoration, etc.

In this preliminary study, it has been shown that low-melting point glasses belonging to the P_2O_5–CaO–Na_2O system (free of highly polluting heavy metals, such as Pb, and with a non-toxic chemical composition, totally compatible with the environment) with an appropriate compositional design can be used in both the field of traditional ceramics and the field of technical ceramics. Considering that a significant application of low melting glasses free of Pb is in the field of decorative ceramics, it is important to point out that the addition of 1 wt.% of Co_2O_3 in the glassy matrix original free of SiO_2, induced an intense blue colour (Fig. 5), as it has been reported in the literature for commercial non-toxic and traditional silicoaluminate based glazes [32–34]. As far as we know, no data have been reported in literature on this topic in P_2O_5–CaO–Na_2O glasses free of silica.

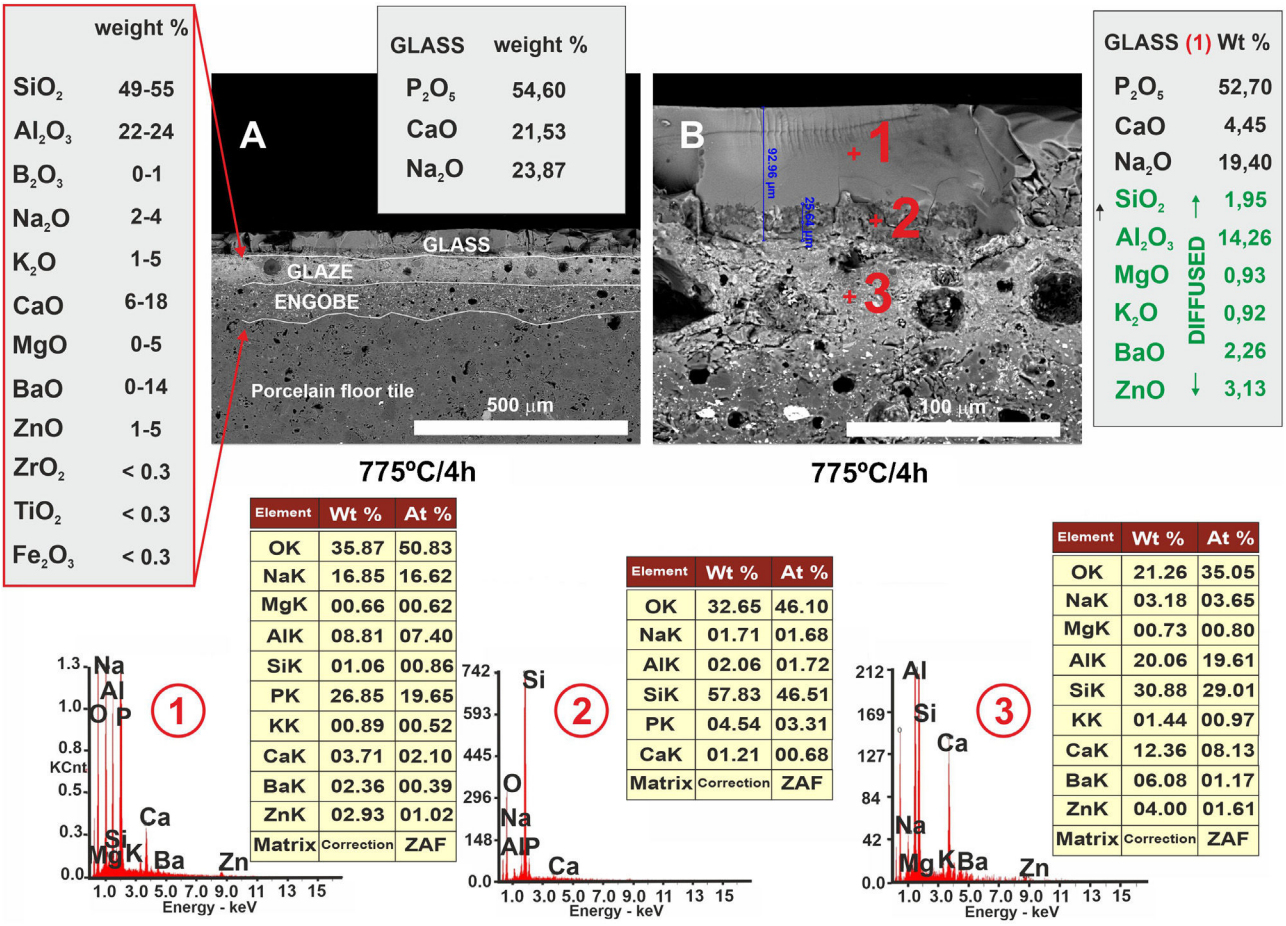

Fig. 10 – FESEM micrographs and EDX microanalyses corresponding to the cross section of the glass/porcelain tile treated at 775 °C/4 h. In the EDX microanalysis of the glass layer (1), the cations incorporated which are not present in the original glass composition are marked as green in the list.

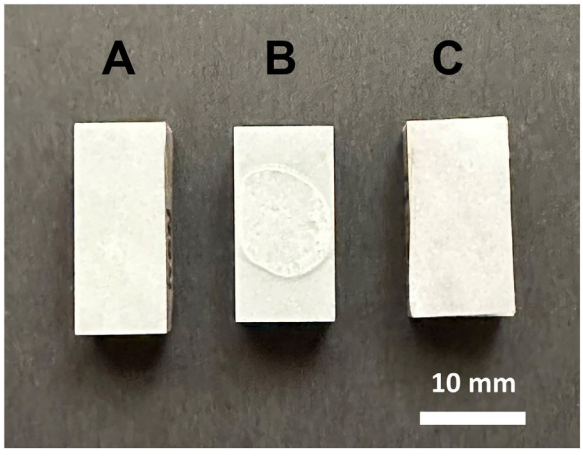

Fig. 11 – Chemically attacked porcelain tiles with the glass coating thermally treated at 875 °C/4 h. The glass coatings were more exposed to hydrochloric acid attack (A) and less sensitive to the citric acid (B) and the alkaline one (C).

Conclusions

The following conclusions can be stated:

1. Starting from a low-melting point glass belonging to the P_2O_5–CaO–Na_2O system, free of heavy metals such as Pb, glassy coatings can be manufactured at 775-875 °C, which is the temperature range commonly used in the ceramic industry for the application of decorative coatings. The glassy coatings obtained exhibit good chemical compatibility and mechanically integrity with both traditional ceramic substrates (porcelain tiles) and technical ceramics (zirconia).
2. During the heat treatment, an ionic exchange takes place with the substrate, that modifies (a) the chemical composition (i.e., in the case of ceramic tiles or alumina dense substrates), as well as (b) the phase relationship of the original glassy coating through nucleation and growth of new phases (i.e., calcium phosphate at the interface in Mg–ZrO_2

substrates) which would improve both its chemical stability and its mechanical stability.
3. We understand that this fact opens up a panoply of application possibilities for these Pb-free low-melting-temperature glasses, both in the field of microelectronics and traditional ceramics.

Acknowledgements

The authors acknowledge the financial support of PID2021-128548OB-C22 project and PID2020-119130GB-I00 project funded by the Spanish *Ministerio de Ciencia e Innovación* (MCIN) and *Agencia Estatal de Investigación* (AEI, MCIN/AEI/10.13039/501100011033), as well as the financial support of CSIC under grant 201960E103 and from FICYT (IDI/2021/000106).

REFERENCES

[1] R. Knechtel, Glass frit bonding: an universal technology for wafer level encapsulation and packaging, Microsyst. Technol. 12 (1–2) (2005) 63–68.
[2] M. Abtew, G. Selvaduray, Lead-free solders in microelectronics, Mater. Sci. Eng. R Rep. 27 (5–6) (2000) 95–141.
[3] Nippon Electric Glass Co., Ltd. https://www.ep.neg.co.jp/en-powder-glass02?gclid=EAIaIQobChMIxc_A1qiB_QIViZBoCR3UyQAEAAYASAAEgJnX_D_BwE.
[4] A.P. Ghosh, L.J. Gerenser, C.M. Jarman, J.E. Fornalik, Thin-film encapsulation of organic light-emitting devices, Appl. Phys. Lett. 86 (22) (2005) 223503.
[5] R. Knechtel, M. Wiemer, J. Frömel, Wafer level encapsulation of microsystems using glass frit bonding, Microsyst. Technol. 12 (5) (2005) 468–472.
[6] M.M. Torunbalci, S.E. Alper, T. Akin, Wafer level hermetic sealing of MEMS devices with vertical feedthroughs using anodic bonding, Sens. Actuator. A Phys. 224 (2015) 169–176.
[7] D. Seo, J. Jeong, T. Kim, J. Lee, A MEMS glass membrane igniter for improved ignition delay and reproducibility, Sens. Actuator. A Phys. 258 (2017) 22–31.
[8] T. Maeder, Review of Bi_2O_3 based glasses for electronics and related applications, Int. Mater. Rev. 58 (1) (2013) 3–40.
[9] Eu-Directive 2002/96/Ec: waste electrical and electronic equipment (WEEE), Off. J. Eur. Union 46 (2003) 24–38.
[10] RoHS Compliance Engineer R, Directive 2002/95/EC of the European Parliament and of the Council of 27 January 2003 on the restriction of the use of certain hazardous substances in electrical and electronic equipment, Off. J. Eur. Union 37 (2005) 19–23.
[11] E. Sánchez, J. García-Ten, V. Sanz, A. Moreno, Porcelain tile: almost 30 years of steady scientific-technological evolution, Ceram. Int. 36 (2010) 831–845.
[12] A. Mezquita, J. Boix, E. Monfort, G. Mallol, Energy saving in ceramic tile kilns: cooling gas heat recovery, Appl. Therm. Eng. 65 (2014) 102e110.
[13] W. Liu, J. Sanz, C. Pecharroman, I. Sobrados, S. Lopez-Esteban, R. Torrecillas, De-Yi Wang, J.S. Moya, B. Cabal, Synthesis, characterization and applications of low temperature melting glasses belonging to P_2O_5–CaO–Na_2O system, Ceram. Int. 45 (2019) 12234–12242.
[14] S. Lopez-Esteban, B. Cabal, A. Borrell, J.F. Bartolomé, A. Fernandez, M. Faraldos, A. Bahamonde, J.S. Moya, C. Pecharroman, Lead-free low-melting-point glass as bonding agent for TiO_2 nanoparticles, Ceram. Int. 47 (2021) 6114–61201.
[15] R. Morena, Phosphate glasses as alternatives to Pb-based sealing frits, J. Non Cryst. Solids 263–264 (2000) 382–387.
[16] J. Cha, T. Kubo, H. Takebe, M. Kuwabara, Compositional dependence of properties of SnO–P_2O_5 glasses, J. Ceram. Soc. Jpn. 116 (2008) 915–919.
[17] R.K. Brow, D.R. Tallant, Structural design of sealing glasses, J. Non Cryst. Solids 222 (1997) 396–406.
[18] H. Masai, M. Takahashi, Y. Tokuda, T. Yoko, Gel-melting method for preparation of organically-modified siloxane low-melting glasses, J. Mater. Res. 20 (2005) 1234–1241.
[19] D. Ehrt, Effect of OH-content on thermal and chemical properties of SnO–P_2O_5 glasses, J. Non Cryst. Solids 354 (2008) 546–552.
[20] H. Takebe, M. Kuwabara, M. Komori, N. Fukugami, M. Soma, T. Kusuura, Imprinted optical pattern of low-softening phosphate glass, Opt. Lett. 32 (2007) 2750–2752.
[21] A. Hayashi, T. Konishi, K. Tadanaga, T. Minami, M. Tatsumisago, Preparation and characterization of SnO–P_2O_5 glasses as anode materials for lithium secondary batteries, J. Non Cryst. Solids 345 (2004) 478–483.
[22] J. Yang, Q. Li, C. Ding, L. He, L. Xue, W. Cheng, Z. Zhang, G. Wei, Y. Liu, L. Huang, Y. Xi, X. Lu, Utilization of B_2O_3-Bi_2O_3–ZnO low-temperature glass-ceramics to immobilize iodine-loaded silver-coated silica-gel, J. Mater. Chem. C 9 (2021) 10462.
[23] D. Kim, J. Lee, J. Huh, H. Kim, Thermal and electrical properties of BaO–B_2O_3–ZnO glasses, J. Non-Cryst. Solids 306 (2002) 70–75.
[24] H. Masai, T. Nishibe, S. Yamamoto, T. Niizuma, N. Kitamura, T. Akai, T. Ohkubo, M. Yoshida, Low melting oxide glasses prepared at a melt temperature of 500 °C, Sci. Rep. 11 (2021) 214.
[25] M.P. Gómez-Tena, A. Moreno, E. Bou, S. Cook, M. Galindo, Use of a new borate raw material for glaze formulation, Boletin de la Sociedad Espanola de Ceramica y Vidrio 49 (4) (2010) 319–326.
[26] UNE-EN ISO 10545-13, July 2017. Baldosas cerámicas, Parte 13: Determinación de la resistencia química. (ISO 10545-13:2016).
[27] M.L.F. Nascimento, E.D. Zanotto, Diffusion processes in vitreous silica revisited, Phys. Chem. Glasses 48 (4) (2007) 201–217.
[28] A.E. Marino, S.R. Arrasmith, L.L. Gregg, S.D. Jacobs, Guorong Chen, Duc. Yongjuan, Durable phosphate glasses with lower transition temperatures, J. Non-Cryst. Solids 289 (1–3) (2001) 37–41.
[29] J. Requena, J.F. Bartolomé, J.S. Moya, S. De Aza, F. Guitian, G. Thomas, Mullite–aluminosilicate glassy matrix substrates obtained by reactive coating, J. Eur. Ceram. Soc. 16 (1996) 249–254.
[30] Y. Iqbal, W. Edward Lee, Microstructural evolution in triaxial porcelain, J. Am. Ceram. Soc. 83 (12) (2000) 3121–3127.
[31] Q. Shia, Y. Yuea, Y. Qua, S. Liua, G.A. Khaterc, L. Zhanga, J. Zhaoa, J. Kang, Structure and chemical durability of calcium iron phosphate glasses doped with La_2O_3 and CeO_2, J. Non-Cryst. Solids 516 (2019) 50–55.
[32] J. Pérez-Arantegui, B. Montull, M. Resano, J.M. Ortega, Materials and technological evolution of ancient cobalt-blue-decorated ceramics: pigments and work patterns

in tin-glazed objects from Aragon (Spain) from the 15th to the 18th century AD, J. Eur. Ceram. Soc. 29 (2009) 2499–2509.
[33] M. Llusar, A. Forés, J.A. Badenes, J. Calbo, M.A. Tena, G. Monrós, Colour analysis of some cobalt-based blue pigments, J. Eur. Ceram. Soc. 21 (2001) 1121–1130.
[34] A. Campanile, B. Liguori, O. Marino, G. Cavaliere, V. Luca De Bartolomeis, D. Caputo, Facile synthesis of nanostructured cobalt pigments by Co–A zeolite thermal conversion and its application in porcelain manufacture, Sci. Rep. 10 (2020) 10147.